

Using OpenFOAM Multiphase Solver interFoam for Large Scale Modeling

A. I. Kurbanaliev, A. R. Maksutov, G. S. Obodoeva and B. R. Oichueva

Abstract—The results of the evaluation of OpenFOAM 6.0 multiphase flows solver interFoam were presented in this paper. A modelling method is based on the three dimensional unsteady Reynolds-averaged Navier-Stokes equations. The volume of fluid method is used for water-air phase interface capturing. The adequacy of the mathematical model is verified by comparison with the corresponding experimental data. The efficiency of used modelling technology was illustrated on the examples of possible flooding flows on the Willow Creek terrain, California, USA and Kara-Daria River area near Jalal-Abad town, Kyrgyzstan.

Index Terms—Dam break flooding, multiphase flow, OpenFOAM, volume of fluid method.

I. INTRODUCTION

The study of the hydrodynamics of river flow is of great practical importance in solving engineering riverside protection problems and predicting the consequences of possible dam-break flooding flows. One of the main aim of mathematical modelling prediction is the determination of the area of propagation of a dam-break wave, which uses various existing methods of modelling the entire flooding process. On the basis of mathematical modelling, in principle, it is possible to make a prediction of the propagation of dam-break waves, to calculate the possible boundaries of the flooding area, the flow rates of floods and water levels at various points in the downstream area. Based on the data of numerical calculations, it is possible to determine the parameters of the necessary engineering riverside protection structures, as well as to estimate the economic losses during flooding and the development of necessary measures against flooding. Until recently, a lot of work on mathematical modelling of the problem of prediction of dam-break waves was based on the numerical solution of Saint-Venant or shallow water equations [1, 2].

Manuscript received July 19, 2019; revised July 30, 2019. This work was supported in part by the Ministry of Education and Sciences of Kyrgyzstan. Abdikerim Kurbanaliev is with the Natural Science and Mathematics Department, Osh State University, Kyrgyzstan, Osh, 723500, Lenina, 331 (phone: +996-779-707-112; fax: +996-322-224-066; e-mail: abdikermkurbanaliev@gmail.com, IAENG Member Number: 14475).

A. R. Maksutov is with Branch of the Russian State Social University in Osh, 723506, Kyrgyz Republic, Osh, Karasu, 161 (e-mail: maksutov_1973@bk.ru).

G. S. Obodoeva is with the Informatics Department, Osh State University, Kyrgyzstan, Osh, 723500, Lenina, 331 (e-mail: obodoevag@mail.ru).

B. R. Oichueva with the Natural Science and Mathematics Department, Osh State University, Kyrgyzstan, Osh, 723500, Lenina, 331 (e-mail: oichuevab@gmail.com).

Authors thanks the Ministry of Education and Sciences of Kyrgyzstan for partial financial support of this work.

Most of them were done in 1D or 2D approximation, but there are a few papers which were done in 3D simulation [3-5]. Herein three-dimensional non-stationary modelling has been performed to simulate such kind of flooding problems by using open source package OpenFOAM [6].

OpenFOAM is designed for numerical simulation of a wide range of tasks related to fluid flow and heat transfer. It contains written in C++ a wide range of crucial and necessary quantities of libraries.

II. MATHEMATICAL MODEL

The three-dimensional mathematical model of the turbulent incompressible flow without of external body forces is based on the Reynolds-averaged Navier-Stokes equations [7, p. 293]:

$$\frac{\partial(\rho u_i)}{\partial x_i} = 0; \quad (1)$$

$$\frac{\partial}{\partial t}(\rho u_i) + \frac{\partial}{\partial x_j}(\rho u_i u_j + \overline{\rho u_i' u_j'}) = -\frac{\partial p}{\partial x_i} + \frac{\partial \tau_{ij}}{\partial x_j} \quad (2)$$

where u_i are the mean velocity components, μ is molecular dynamic viscosity, ρ is density, $\tau_{ij} = \mu \left(\frac{\partial u_i}{\partial x_j} + \frac{\partial u_j}{\partial x_i} \right)$ are mean viscous stress tensor components and $\overline{\rho u_i' u_j'}$ are Reynolds-stress tensor. The averaging is done in time, and the prime denotes the fluctuation part of the velocity. In the presence of external body forces, it is necessary to augment these equations by the corresponding terms.

Turbulent viscosity, which relates to the mean velocity flow gradients, can be written in the following form of eddy-viscosity model [7, p. 294]:

$$-\overline{\rho u_i' u_j'} = \mu_t \left(\frac{\partial u_i}{\partial x_j} + \frac{\partial u_j}{\partial x_i} \right) - \frac{2}{3} \rho \delta_{ij} k$$

In this paper the closure of systems of equations (1-2) is based on the standard k - ε - model of turbulence. The kinetic energy of turbulence and its dissipation rate ε are calculated by following transport equations [7, pp. 295-296]:

$$\frac{\partial(\rho k)}{\partial t} + \frac{\partial(\rho u_j k)}{\partial x_j} = \frac{\partial}{\partial x_j} \left[\left(\mu + \frac{\mu_t}{\sigma_k} \right) \frac{\partial k}{\partial x_j} \right] + P_k - \rho \varepsilon$$

$$\frac{\partial(\rho \varepsilon)}{\partial t} + \frac{\partial(\rho u_j \varepsilon)}{\partial x_j} = C_{\varepsilon 1} P_k \frac{\varepsilon}{k} - \rho C_{\varepsilon 2} \frac{\varepsilon^2}{k} + \frac{\partial}{\partial x_j} \left[\frac{\mu_t}{\sigma_\varepsilon} \frac{\partial \varepsilon}{\partial x_j} \right]$$

where $P_k = \mu_t \left(\frac{\partial u_i}{\partial x_j} + \frac{\partial u_j}{\partial x_i} \right) \frac{\partial u_i}{\partial x_j}$ is the rate of production of turbulent kinetic energy by the mean flow, $\mu_t = \rho C_\mu \frac{k^2}{\varepsilon}$ is eddy viscosity. This k- ε model of turbulence has next five most used coefficients: $C_\mu = 0.09; C_{\varepsilon_1} = 1.44; C_{\varepsilon_2} = 1.92; \sigma_k = 1.0; \sigma_\varepsilon = 1.3$.

A. PHASE INTERFACE CAPTURING

Flows with free surfaces are very complicated ones with moving boundaries. As usual, the location of the boundary is known only at the beginning of time and its position at later times has to be determined as a part of the numerical solution.

The method of determining the interface between immiscible two phases — water and air occupies special place during the modelling of the multiphase flow. According to the main idea of the volume of fluid method (VOF) [7, p. 384], for each computational cell one determines a scalar quantity, which represents the degree of filling of the cell with one phase, for example, water. If this quantity is equal to 0, computational cell is empty; if this quantity is equal to 1, then the computational cell is filled completely. If its value lies between 0 and 1, then one can say, respectively, that this cell contains the free (interphase) boundary. In other words, the volume fraction of water α is determined as the ratio of the water volume in the cell to the total volume of the given cell. The quantity $1 - \alpha$ represents, respectively, the volume fraction of the second phase — air in the given cell. At the initial moment of time, one specifies the distribution of the field of this quantity, and its further temporal and spatial evolutions are computed from the following transport equation [7, p. 384]:

$$\frac{\partial \alpha}{\partial t} + \frac{\partial(\alpha u_i)}{\partial x_i} = 0.$$

The free boundary location is determined by the equation $\alpha(x, y, z, t) = 0$. Therefore, the physical properties of the gas-liquid mixture are determined by averaging with the corresponding weight coefficient [7, p. 385]: $\rho = \alpha \rho_1 + (1 - \alpha) \rho_2$, $\mu = \alpha \mu_1 + (1 - \alpha) \mu_2$. Here the subscripts 1 and 2 refer to the liquid and gaseous phases.

The essence of the VOF method implemented in the solver interFoam of the OpenFOAM package [1] lies in the fact that the interface between two phases is not computed explicitly, but is determined, to some extent, as a property of the field of the water volume fraction. Since the volume fraction values are between 0 and 1, the interphase boundary is not determined accurately, however, it occupies some region, where a sharp interphase boundary must exist in the proximity.

B. MESH GENERATION

It is well known that very important pre-processing problem is generation of an appropriate mesh. The flow considered in this paper is reasonably complex and an

optimum solution will require grading of the mesh. In general, the regions of highest shear are particularly critical, requiring a finer mesh than in the regions of low shear. For this purpose, we use a full mesh grading capability of blockMesh and snappyHexMesh utilities of the OpenFOAM.

For regions with complicated topography data terrain the topography data of Digital Terrain Elevation Data [8] were used in computations, which were converted subsequently into the Stereolithography (STL) format. First of all, by the simple using blockMesh, it is necessary to create a background the hexahedral background mesh that fills the entire region within by the external boundary.

Then the snappyHexMesh utility used for generating 3D mesh containing hexahedra and split-hexahedra automatically from tri-surfaces in STL format. The mesh approximately conforms to the surface by iteratively refining a starting background mesh and morphing the resulting split-hex mesh to the surface in STL format. An optional phase will shrink back the resulting mesh and insert cell layers. The specification of mesh refinement level is very flexible and the surface handling is robust with a pre-specified final mesh quality [6].

C. INITIAL CONDITIONS

For the unsteady problem, it is necessary to specify for the initial values for all dependent variables. The values of all velocity components are equal to zero because according to the initial condition of the problem, there is no motion until the moment of time $t = 0$. The hydrodynamic pressure is also equal to zero since the used solver – interFoam calculates hydrodynamic pressure [6]. The turbulence kinetic energy and its dissipation rate have some small value, which ensures a good convergence of the numerical solution at the first integration steps. The initial values for k and ε are set using an estimated fluctuating component of velocity U' and a turbulent length scale. The initial distribution of the phase fraction of water α is non-uniform because not all the computational cells are filled with water.

D. BOUNDARY CONDITIONS

The no-slip condition is specified at solid walls of the computational region, which gives the zero components of the velocity vector. The Neumann conditions are specified for the water volume fraction: and $\frac{\partial \alpha}{\partial n} = 0$. At all solid wall boundaries, the fixedFluxPressure boundary condition is applied to the pressure (hydrodynamic pressure) field, which adjusts the pressure gradient so that the boundary flux matches the velocity boundary condition for solvers that include body forces as gravity and surface tension [6].

The boundary conditions for the turbulence kinetic energy k and its dissipation rate ε were specified with the aid of wall functions [7, p.298]. Systematic calculations performed in this work show that the minimum value of dimensionless distance y^+ for all solid wall greater than 25, so we can use wall functions technique.

In all flows considered in this paper, one is only interested in modelling the inner-region. There is no specific need in

resolving the viscous layer. The use of wall functions is convenient in this context for avoiding extra refining of the mesh near the solid walls and reducing the computational cost [7, p. 298].

The influence of surface tension forces between the solid wall and the gas-liquid mixture were not taken into account in this paper.

The top boundary is free to the atmosphere so needs to permit both outflow and inflow according to the internal flow. That is why it is necessary to use a combination of boundary conditions for pressure and velocity that does this while maintaining stability.

E. METHODS FOR DISCRETIZATION AND SOLVING SYSTEM OF LINEAR EQUATIONS

For numerical solution of the system of equations (1-2), it is necessary to carry out a discretization procedure, the purpose of which is to convert the system of partial differential equations (1-2) into a system of linear algebraic equations. The solution of this system determines a certain set of quantities that are of particular relevance to the solution of the initial differential equations at certain points in space and time. The general discretization procedure consists of two stages: spatial discretization and equation discretization.

Spatial discretization is carried out on the basis of the control volume method [8, p. 30]. According to the basic idea of this method, the spatial discretization of the problem is obtained by dividing the computational domain into a finite number of contiguous volumes. In the center of each control volume there is only one point of “binding” of the numerical solution. In most developments focused on solving three-dimensional problems for areas of complex geometry, the computational grid cells are used as the control volume: the grid nodes are located at the vertices of the polyhedron, the grid lines go along its edges, and the values of the desired quantities are assigned to the geometric center of the cell.

The system of differential equations is linearized and sampled for each control volume. To calculate the volume integrals over the control volume, the general Gauss theorem was used, according to which the volume integral is represented through the integral over the cell surface, and the function value on the surface is interpolated from the function values in the centroids of the neighboring cells.

As a discrete time discretization scheme, an explicit first-order Euler scheme was used with backward differences. For the associated calculation of the velocity and pressure fields, the PISO procedure with the number of correctors 3 was used [7, p. 178]. To solve the obtained system of linear algebraic equations, iterative PCG solvers for symmetric matrices [7, p.107] and PBiCG method (bi-) conjugate gradients with preconditioning for asymmetric matrices [7, p.110] were used. As a preconditioner, the DIC preconditioner procedures were chosen based on the simplified scheme of incomplete Cholesky factorization for symmetric matrices and DILU preconditioner based on simplified incomplete LU factorization for asymmetric matrices.

III. DAM-BREAK FLOW MODELING IN REAL REGION

To illustrate the techniques of the application of numerical modelling of large-scale hydrodynamic computations we consider the problem of computing the flood process in the Willow Creek Mountain Area, USA [9], which terrain is presented on Fig.1.

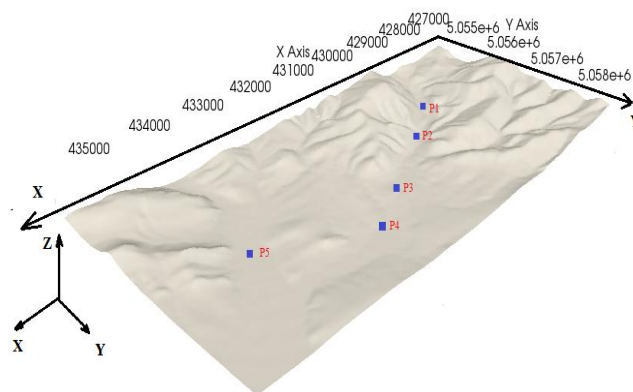


Fig. 1. Willow Creek terrain.

The coordinates of five probes are given in the Table 1.

Table 1. Probe locations

Probe #	X, m	Y, m	Z, m
Point1	428728.8	5055327.9	1750.85
Point2	429675.63	5055941.98	1700
Point3	431142.22	5056648.3	1656
Point4	432056.65	5057154	1615
Point5	433876.18	5056278.4	1596.8

It is to be emphasized here that the situation of a real breakthrough of the dam and the flood of the areas at the lower level is not modeled here but the fundamental possibility of using the above technology under the availability of necessary topography data is demonstrated. The topography data of Willow Creek used in these computations, were taken from US Geological Survey [10] and were converted subsequently into the stl format. The hexahedral background grid generated with the aid of the utilities blockMesh and snappyHexMesh of the OpenFOAM package was transformed into a three-dimensional surface, which is employed for modeling the flood process (Fig. 1). Final total number of computational cells after using snappyHexMesh utility equal to 450705. The computations were done in this case on computer Intel® Core i5-8250U CPU @1.60 GHz with 8Gb installed operating memory. Total simulations time on this computer takes 17934 s which is almost 5 hours.

The distributions of volume fraction of water at different time moments are presented on Fig.3-Fig.5.

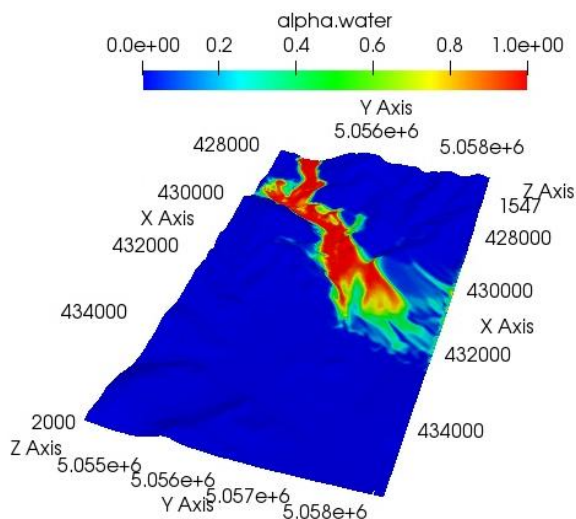


Fig. 2. Volume of Water distribution at t=20s.

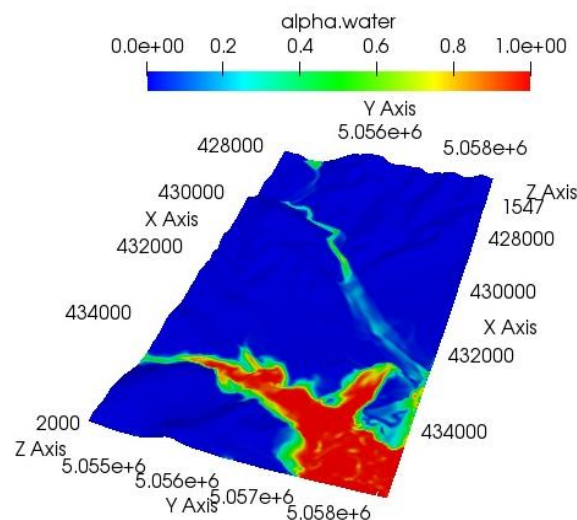


Fig. 5. Volume of Water distribution at t=80s.

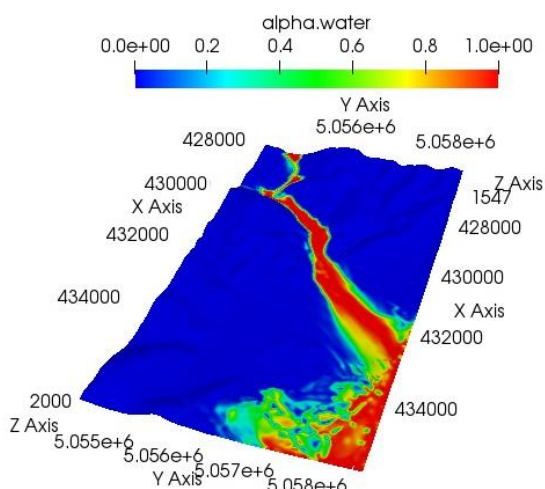


Fig. 3. Volume of Water distribution at t=40s.

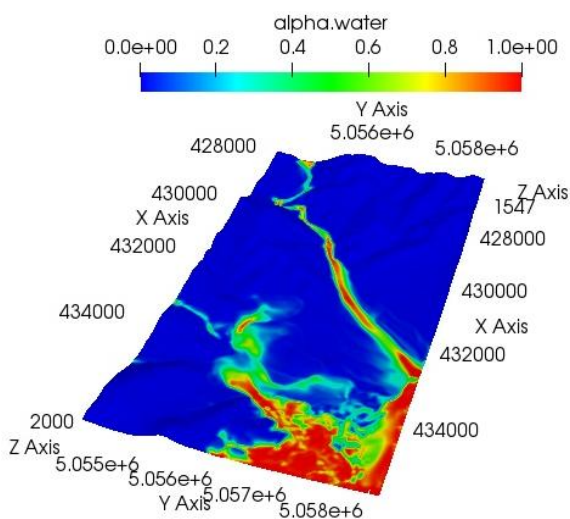


Fig. 4. Volume of Water distribution at t=60s.

The red color corresponds to a pure water flow, and the blue color corresponds to air flow (there is no water flow in blue regions).

Variations of water height at different points P1-P5 are presented next Fig. 6-Fig.10.

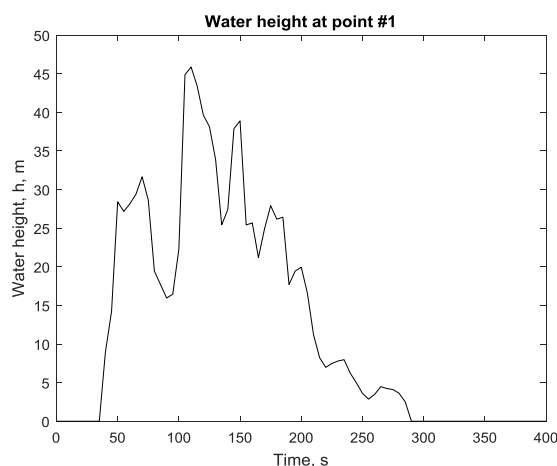


Fig. 6. Water height at P1.

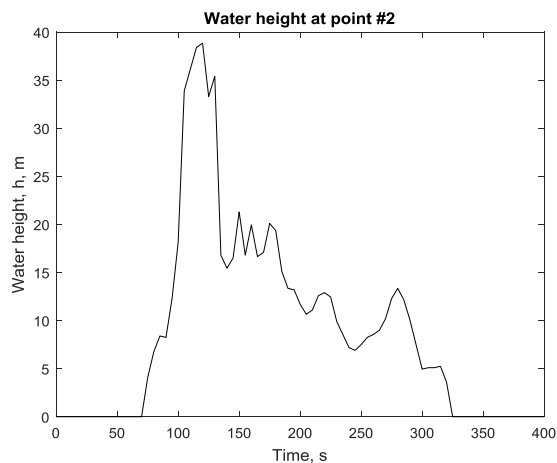


Fig. 7. Water height at P2.

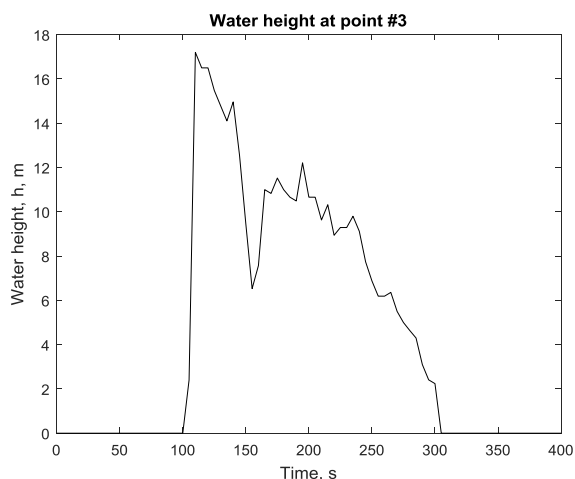


Fig. 8. Water height at P3.

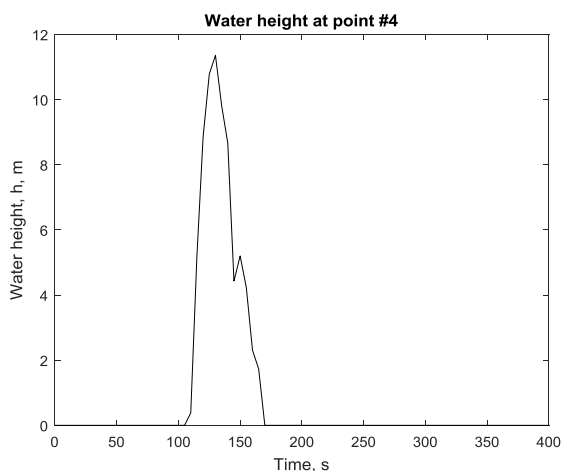


Fig. 9. Water height at P4.

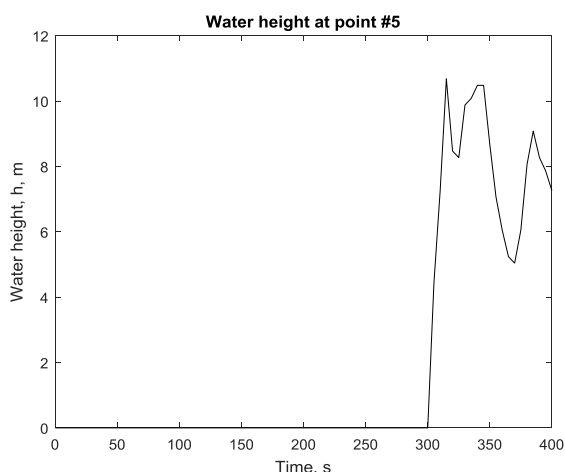


Fig. 10. Water height at P5.

The present work does not account for the interaction of water flow with river-bed flora and various structures, which change significantly the general flow pattern leading to a flood zone increase.

IV. CONCLUSION

This paper presents the numerical investigation of dam-break wave propagation during initial stages in a 3D real terrain – Willow Creek Mountain area, California, USA.

The interFoam solver of open software OpenFOAM was used for numerical simulation.

Unsteady three-dimensional Navier—Stokes equations describing the dynamics of a gas-liquid mixture with free boundary were as a basis of the mathematical modeling of complex large scale hydrodynamic phenomena.

It is necessary to note specially that due to the limitations of the computer computational resources the computing mesh size was chosen relatively crude. Therefore, one must consider the presented computational results as the estimation ones, they need verification on a finer mesh.

REFERENCES

- [1] W. Lai, A. Khan. 2018. Numerical solution of the Saint-Venant equations by an efficient hybrid finite-volume/finite-difference method. *Journal of Hydrodynamics*. 30(4), (2018) DOI: 10.1007/s42241-018-0020-y.
- [2] X. Ying, J. Jorgenson, S. S. Y. Wang. 2008. Modelling Dam-Break Flows Using Finite Volume Method on Unstructured Grid. *Journal of Engineering Application of Computational Fluid Mechanics*. 3:2, 184-194, <https://doi.org/10.1080/19942060.2009.11015264>.
- [3] R. Issa, D. Vouleau. 2006. 3D dambreaking. SPH European Research Interest Community SIG, Test case 2; March, 2006. Available from: http://app.spheric-sph.org/sites/spheric/files/SPHERIC_Test2_v1p1.pdf. [Accessed: 2019-04-15].
- [4] A. Zh. Zhainakov, A.Y. Kurbanaliev. 2013. Verification of the open package OpenFOAM ob dam break problems. *Thermophysics and Aeromechanics*. 20(4), (2013) DOI: [10.1134/S0869864313040082](https://doi.org/10.1134/S0869864313040082).
- [5] A. Lindsey, J. Imran, M. Chfudhry. 3D numerica simulation of partial breach dam-break flow using the LES and k-ε- turbulence models. *Journal of Hydraulic Research*. (2013). <https://doi.org/10.1080/00221686.2012.734862>.
- [6] OpenFOAM Foundation. 2018. Available from: <https://openfoam.org/> [Accessed: 2019-03-30].
- [7] H. Ferziger and M. Peric, *Computational Methods for Fluid Dynamics*. 3rd Edition. Springer Verlag, Berlin, 2002. DOI: 10.1007/978-3-642-56026-2.
- [8] S.V. Patankar, *Numerical Heat Transfer and Fluid Flow*, Hemisphere Publ. Corp., New York, 1980. <https://doi.org/10.1002/cite.330530323>.
- [9] Willow Creek California, USA https://en.wikipedia.org/wiki/Willow_Creek,_California. [Accessed: 2019-02-20].
- [10] United States Geological Survey United States Topo 7.5-minute map for Willow Creek, CA 2012. <https://www.sciencebase.gov/catalog/item/58260258e4b01fad86e73226>, [Accessed: 2019-02-20].